Structural Characteristic Analysis of a High-precision Centerless Grinding Machine with a Concrete-filled Bed

Seok-Il Kim[1,#] and Jae-Wan Cho[2]

1 School of Aerospace and Mechanical Engineering, Hankuk Aviation University, Goyang-Si, Gyeonggi-Do, South Korea
2 Graduate School, Hankuk Aviation University, Goyang-Si, Gyeonggi-Do, South Korea
Corresponding author / E-mail: sikim@hau.ac.kr, Tel: +82-2-300-0176, Fax: +82-2-3158-4231

KEYWORDS : High-precision centerless grinding machine, Concrete-filled bed, Grinding wheel, Regulating wheel, Loop stiffness, Ferrule

High-precision centerless grinding machines are emerging as a means of finishing the outer diameter grinding process required for ferrules, which are widely used as fiber optic connectors. In this study, a structural characteristic analysis and evaluation were carried out using a virtual prototype of a centerless grinding machine to realize systematic design technology and performance improvements required to manufacture ferrules. The prototype consisted of a concrete-filled bed, hydrostatic grinding wheel (GW) and regulating wheel (RW) spindle systems, a hydrostatic RW feed mechanism, a RW swivel mechanism, and on-machine GW and RW dressers. The loop stiffness values of the centerless grinding machine were estimated based on the relative displacements between the GW and RW caused by grinding forces. The simulated results illustrated that a concrete-filled bed considerably improved the structural stiffness and accuracy of a high-precision centerless grinding machine.

Manuscript received: February 1, 2006 / Accepted: February 9, 2006

1. Introduction

A centerless grinding machine can grind inner and outer cylindrical surfaces without chucking or centering the workpiece. It is therefore a highly productive machine that is able to produce precision products easily regardless of the skill of the operator.[1,2] Thus, high-precision centerless grinding machines are emerging as more efficient finishing tools for the outer diameter grinding process of high-precision ferrules,[3] which affects the transmission efficiency and quality of optical communications.

In general, ferrules are made from zirconia (ZrO_2), which is a ceramic material. Most of the required tolerances for ferrules are less than 1 μm, and their outer diameter, concentricity, roundness, and surface roughness are very strictly regulated. If the outer diameter finishing grinding process is performed with a centerless grinding machine, the outer diameter and concentricity are greatly influenced by the axial stiffness and feed accuracy of the regulating wheel (RW) table feed system while the roundness and surface roughness are greatly influenced by the rotational accuracy of the grinding wheel (GW) and RW spindle systems. Therefore, when manufacturing ferrules, high-precision centerless grinding machines are required to have better stiffness and accuracy than machines used for more general work. The comprehensive countermeasures related to the RW table feed system and the GW and RW spindle systems are especially important.

Cho et al.[4] investigated the specifications and functions required to realize a high-precision centerless grinding machine, while Lee et al.[5] manufactured and evaluated the required on-machine wheel dressing system. Park et al.[6] experimentally estimated the stiffness, position accuracy, and repeatability of a hydrostatic feed system for a centerless grinding machine and demonstrated its possible applicability for high-precision machining. However, these studies were only concerned with conceptual investigations or experimental results; a structural analysis study, which systematically identifies problems in the structural design and presents a corresponding design improvement strategy, has not yet been performed.

In this study, the effects of the structural elements on the structural deformation and stiffness of a high-precision centerless grinding machine were estimated in the design stage. The structural characteristic information required at the manufacturing stage was derived from the estimated results to realize systematic design technology and performance improvements required to manufacture ferrules. The influences of the machine weight and grinding forces on the structural deformation were analyzed by constructing a virtual prototype of a centerless grinding machine. The loop stiffness values were evaluated based on the relative displacements between the GW and RW caused by grinding forces. The causes of structural stiffness deterioration, which are difficult to understand experimentally, were identified from the various structural deformation analysis results. The use of a concrete-filled bed was shown to have a considerable effect on the structural stiffness and accuracy of the centerless grinding machine by comparing the structural characteristics of concrete-filled and unfilled beds.

2. Structural Design of a High-Precision Centerless Grinding Machine

2.1 Grinding Machine

The basic structure of a high-precision centerless grinding machine is presented in Fig. 1. The GW spindle head was mounted directly on the bed, and the RW spindle head, which contained a swivel head that regulated the RW setting angle to determine the workpiece feed rate, was mounted on the feed table. To simplify the machine structure and to enhance the efficiency of the grinding operation, the on-machine GW and RW dressers were mounted behind the GW and RW spindle heads, respectively, and concrete was used to fill the steel bed to obtain a stiff machine structure.

The width and diameter of the GW were set to 150 and 250 mm, respectively, to grind ten ferrules with the specifications shown in Table 1. The width and diameter of the RW were set to 180 and 205 mm, respectively, to ensure sufficient guiding accuracy when the ferrules entered the grinding process. The GW was made from diamond since the ferrules were composed of zirconia.

2.2 Spindle System

The spindle systems of the high-precision centerless grinding machine were separated into GW and RW components. Hydrostatic bearings were used for the spindle bearings because the roundness and surface roughness of the ferrules are greatly influenced by the rotational accuracy of the spindle systems. The stiff spindle systems required to minimize the displacement of the wheels due to the grinding load were realized by installing the GW and RW between left and right hydrostatic journal bearings. Fig. 2 shows a schematic diagram of the hydrostatic journal bearings, and the design specifications are listed in Table 2. The same information for the hydrostatic thrust bearings can be found in Fig. 3 and Table 3.[7]

2.3 Feed System

The outer diameter and concentricity of a ferrule are greatly influenced by the axial stiffness and feed accuracy of the RW table feed system due to the grinding principles of the high-precision centerless grinding machine. Therefore, a hydrostatic guideway and a servo motor-ball screw driving mechanism were used in the feed system. Since most of the grinding load is applied in the axial direction of the RW table feed system, the axial stiffness of the feed system has to be high enough to achieve the required ferrule tolerances. Besides increasing the axial stiffness of the ball screw mechanism, a structural design for decreasing the axial deformation at the connection joints between the ball screw support bearing brackets and the bed is required to increase the axial stiffness of the feed system.

By considering the above factors, a NSK PFT 4006-7.5 with an oversize ball preload was selected as the ball screw for the RW table feed system. Four angular contact ball bearings, NSK 30TAC62, were installed on the servo motor side to act as ball screw support

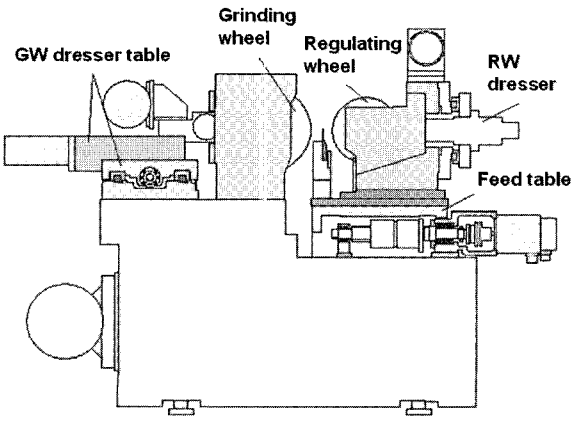

Fig. 1 Schematic diagram of a centerless grinding machine

Table 1 Ferrule specifications

Dimensions	2.5 × 10.5 mm	Accuracy	60.5 μm
Material	ZrO_2	Roundness	0.5 μm
Roughness	0.05 μm R_a	Concentricity	1.0 μm

bearings. The estimated stiffness of the ball screw support bearings K_b, nut K_n, and shaft K_s was 2,011 N/μm, 659 N/μm, and 1,271 N/μm, respectively, when the ball screw nut was located at the standard position for grinding the ferrule.[8,9] Therefore, the estimated overall axial stiffness K_f of the ball screw mechanism was 357 N/μm from the equivalent stiffness equation[8] given by

$$\frac{1}{K_f} = \frac{1}{K_b} + \frac{1}{K_n} + \frac{1}{K_s} \tag{1}$$

The vertical stiffness of the hydrostatic guideway was designed by considering the weights of the RW spindle head and RW dresser mounted on the feed table, as shown in Fig. 1. The horizontal stiffness of the hydrostatic guideway was designed by considering the fact that smaller feed table yaw errors give rise to better ferrule tolerances. Therefore, to improve the stiffness and ease of assembly of the hydrostatic guideway, a reverse confining hydrostatic guideway, in which the rails wrap the double-pad hydrostatic bearings as shown in Fig. 4, was introduced. To improve the feed accuracy, countermeasures for minimizing the elastic deformation of the guideway structure due to the recess pressure of the hydrostatic bearings were required in addition to the left–right symmetric structure design of the feed system. The design specifications of the hydrostatic guideway that were established based on these concepts are presented in Table 4 .[7]

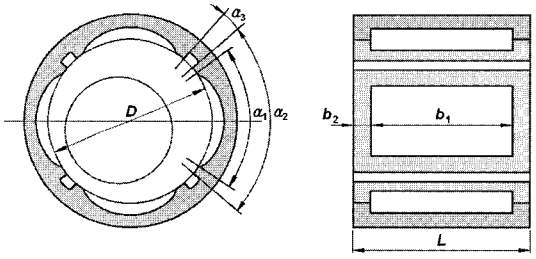

Fig. 2 Schematic diagram of the hydrostatic journal bearings

Table 2 Specifications of the hydrostatic journal bearings

Specifications	GW	RW
Diameter/Length D, L	60, 60 mm	50, 50 mm
Angle α_1, α_2, α_3	63.00, 86.18, 3.82°	62.5, 80.8, 9.2°
Axial length b_1, b_2	48, 6 mm	40, 5 mm
Bearing clearance	20 μm	20 μm
Stiffness	241 N/μm	163 N/μm
Supply pressure	2 MPa	
Dynamic viscosity	5 cSt (40 °C)	

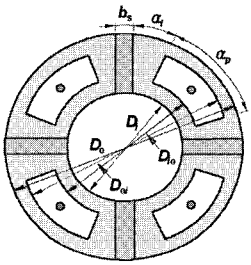

Fig. 3 Schematic diagram of the hydrostatic thrust bearings

Table 3 Specifications of the hydrostatic thrust bearings

Specifications	GW	RW
D_i, D_{io}, D_{oi}, D_o	64, 67, 77, 80 mm	54, 58, 68, 72 mm
Angle α_I, α_p	11.91, 63.00°	11.68, 63.00°
Width b_s	4 mm	4 mm
Bearing clearance	20 μm	20 μm
Stiffness	150 N/μm	143 N/μm
Supply pressure	2 MPa	
Dynamic viscosity	5 cSt (40 °C)	

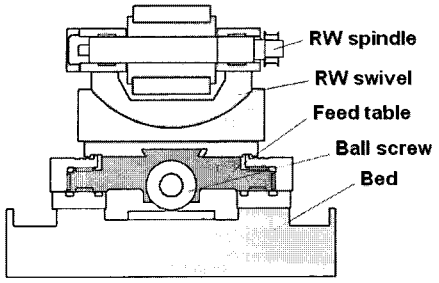

Fig. 4 Hydrostatic guideway structure

Table 4 Specifications of the hydrostatic guideway

Specifications	Horizontal	Vertical
Number of pads	6	12
Pad dimensions	120 × 32 mm	120 × 32 mm
Bearing clearance	25 μm	25 μm
Static stiffness	480 N/μm	960 N/μm
Supply pressure	1 MPa	
Dynamic viscosity	5 cSt (40 °C)	

3. Structural Characteristic Analysis of the High-Precision Centerless Grinding Machine

3.1 Virtual Prototype (Finite Element Model)

A virtual prototype of the high-precision centerless grinding machine was constructed to estimate its structural characteristics, as shown in Fig. 5. The principal structural modules of the virtual prototype are presented in Fig. 6 to better explain the construction of the centerless grinding machine. The virtual prototype consisted of 62,405 nodes, 74,112 solid elements, and 167 matrix elements. The matrix elements were introduced to represent the stiffness values related to the ball screw mechanism and hydrostatic guideway of the RW table feed system (X-axis feed system), the hydrostatic journal and thrust bearings of the GW and RW spindle systems, and the guideways of the GW and RW dressers and ball bearings.

The GW and RW spindles and the bed were made of steel (SS440, SCM435), while the GW and RW spindle housings, the GW and RW dresser housings, and the feed table and rails of the RW table feed system were made of cast iron (GC300). Concrete was used to fill the bed. The material properties are given in Table 5. The mass of each structural module illustrated in Fig. 6 was estimated as follows: 727 kg for the steel bed, 791 kg for the concrete, 265 kg for the RW table feed mechanism (table, rails, ball screw, and bracket), 344 kg for the GW spindle head (spindle and housing), 228 kg for the RW spindle head (spindle and housing), 316 kg for the GW dresser, and 27 kg for the RW dresser. The estimated total mass of the high-precision centerless grinding machine was 2,698 kg.

3.2 Structural Characteristics

3.2.1 Structural Deformation due to Machine Weight

The six supporting points of the bed were rigidly fixed to act as boundary conditions for the centerless grinding machine structural characteristic analysis. Gravity and hydrostatic effects, *i.e.*, the effect of the oil pressure of the hydrostatic bearings, were considered.

The structural deformation of the high-precision centerless grinding machine is illustrated in Fig. 7(a) and (b) in isometric and sectional views. Because the mass center of the structural elements on the RW feed table deviated by 47 mm toward the RW dresser from the table center, the structural elements were rotated clockwise as shown in Fig. 7(b) to create a RW position error. Therefore, the positions of the structural elements on the RW feed table need to be shifted 47 mm toward the GW spindle head in order to solve the problem.

Table 6 compares the vertical deformations of the left and right rails of the concrete-filled and unfilled beds. These were evaluated

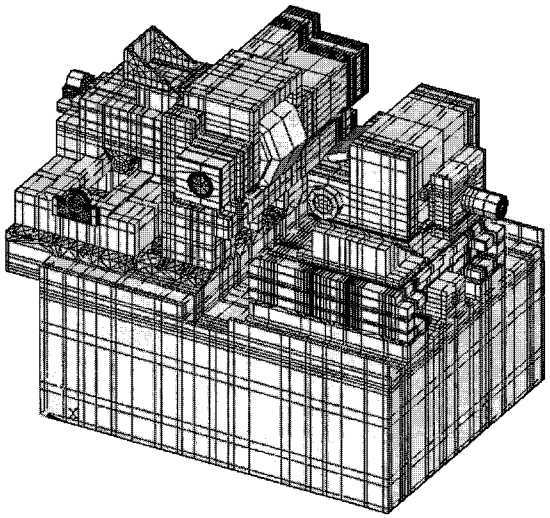

Fig. 5 Virtual prototype of the grinding machine

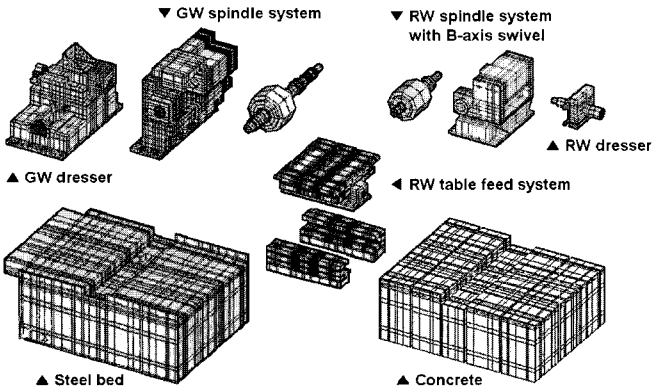

Fig. 6 Structural modules of the virtual prototype

Table 5 Material properties used for the virtual prototype

Steel (SS400)	Young's modulus	200 GPa
	Density	7,850 kg/m^3
	Poisson's ratio	0.32
Steel (SCM435)	Young's modulus	205 GPa
	Density	7,850 kg/m^3
	Poisson's ratio	0.28
Cast iron (GC300)	Young's modulus	90 GPa
	Density	7,300 kg/m^3
	Poisson's ratio	0.25
Concrete	Young's modulus	27 GPa
	Density	2,320 kg/m^3
	Poisson's ratio	0.15

at the measurement points shown in Fig. 8. The predicted maximum deformation of the centerless grinding machine with a concrete-filled bed was 10.1 μm, and occurred at the upper-middle position of the hydrostatic guideway rails. This phenomenon originates from the bending deformation of the rails caused by hydrostatic effects. Due to the bending of the rails, the upper gaps of the left and right

hydrostatic guideways increased on average by 4.15 μm (from 1.25 μm to 7.06 μm) and 4.62 μm (from 1.34 μm to 7.89 μm), respectively, for the concrete-filled bed. The subsequent real vertical stiffness of the hydrostatic guideway was expected to become 865 N/μm (or about 10 %) less than the designed vertical stiffness of 960 N/μm. For the machine with the unfilled bed, the upper gaps of the left and right hydrostatic guideways increased on average by 5.00 μm (from 2.00 μm to 8.00 μm) and 5.74 μm (from 2.33 μm to 9.15 μm), respectively. This demonstrates that the increments in the upper gap of the hydrostatic guideway can be reduced by about 20 %, or 1 μm, by using a concrete-filled bed.

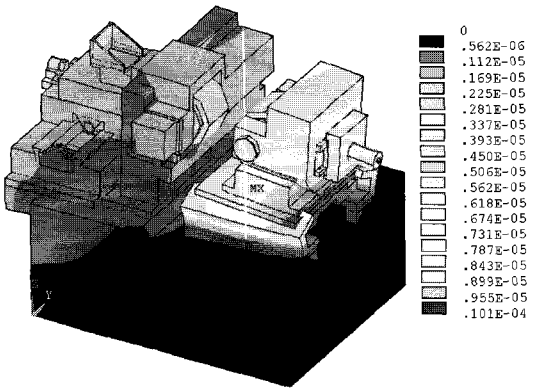

Fig. 7(a) Structural deformation of the virtual prototype due to gravity

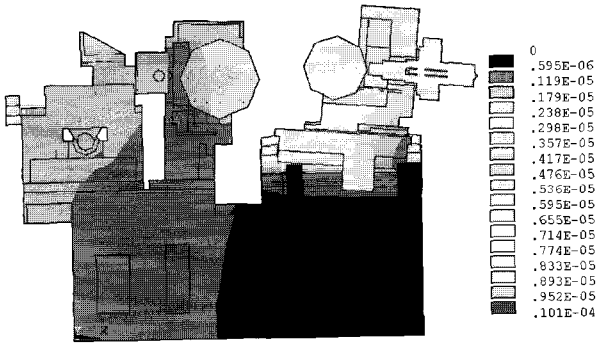

Fig. 7(b) Sectional view of the structural deformation

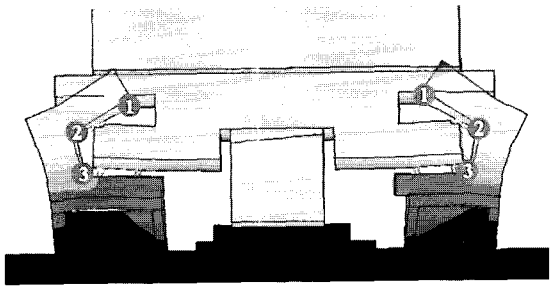

Fig. 8 Measurement points of the hydrostatic guideway

Table 6 Vertical deformation of the hydrostatic guideway

Point	Concrete-filled bed		Unfilled bed	
	Left	Right	Left	Right
1	7.06 μm	7.89 μm	8.00 μm	9.15 μm
2	1.25 μm	1.34 μm	2.00 μm	2.33 μm
3	0.62 μm	0.60 μm	1.38 μm	1.60 μm

The deflections of the upper bed plate measured from left to right along the longitudinal centerline of the bed are presented in Fig. 9. The results show that the left portion of the plate deflected more than the right portion. This is because the left portion, on which the GW dresser (316 kg) and the GW spindle head (344 kg) were mounted, received more load than the right portion, on which the RW table feed mechanism (265 kg), the RW spindle head (228 kg), and the RW dresser (27 kg) were mounted. The deflections of the upper bed plate measured from front to rear along the transverse center line of the beds are presented in Fig. 10. The rear portion of the plate was more deflected than the front portion because the mass center of the GW spindle head, which had a great influence on the deflection, deviated toward the rear portion of the plate. The deflections of the high-precision centerless grinding machine with the unfilled bed were approximately 100 % and 150 % greater in the longitudinal and transverse directions, respectively, than those of the machine with the

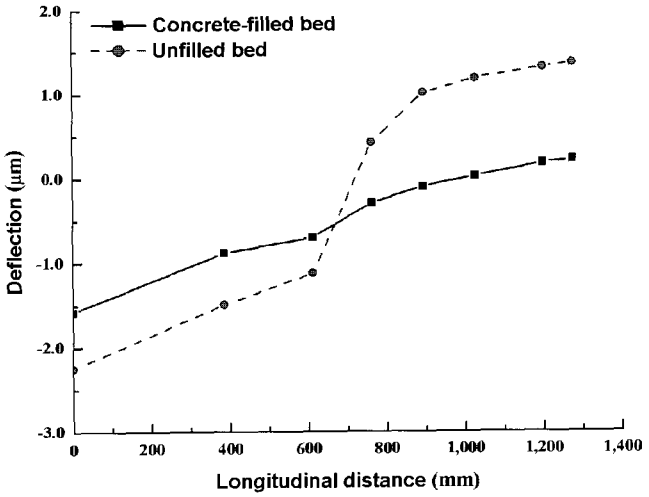

Fig. 9 Deflection of the upper bed plate in the longitudinal direction

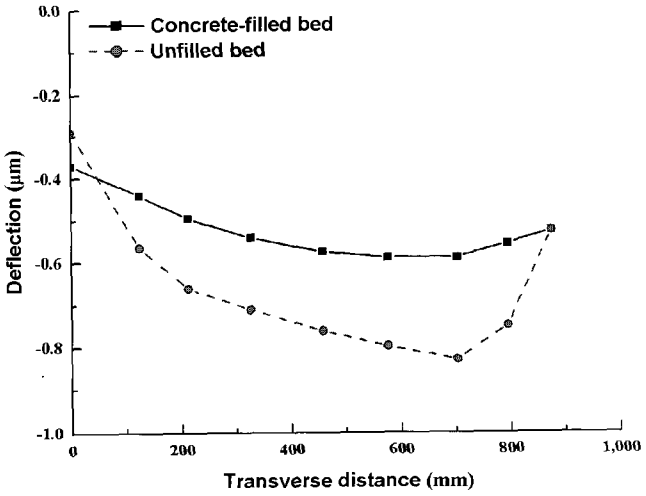

Fig. 10 Deflection of the upper bed plate in the transverse direction

concrete-filled bed. Therefore, the introduction of a concrete-filled bed greatly contributed to an increased structural stiffness of the high-precision centerless grinding machine.

3.2.2 Horizontal Loop Stiffness

The horizontal loop stiffness was estimated by analyzing the structural deformation of the centerless grinding machine when a horizontal grinding force of 1 N in the opposition direction was applied to the center portion of the GW and RW. Fig. 11 shows the structural deformation of the centerless grinding machine caused by the horizontal grinding force, and Table 7 lists the axial and vertical displacements of the RW feed table at the measurement points shown in Fig. 12. The difference between the axial displacement at points 3 (front left portion) and 4 (front right portion) was 0.0 μm. Therefore, the yaw error of the RW feed table caused by the horizontal grinding force was extremely small. This verifies that the RW feed system was designed as a well-balanced left–right symmetric structure. The

pitch error of the RW feed table caused by the horizontal grinding force was proportional to the difference between the vertical displacement at points 1 (front center portion) and 2 (rear center portion). The difference between the vertical displacement at points 1 and 2 was 0.0052 μm with the concrete-filled bed and 0.0057 μm with the unfilled bed. Thus, the pitch error of the RW feed table was reduced by about 10% by introducing a concrete-filled bed.

When a horizontal grinding force of 1 N in the opposition direction was applied to the center portions of GW and RW, the horizontal displacement of the GW and RW were –0.0038 μm and 0.0090 μm, respectively, and the horizontal loop stiffness was 72.5 μm/N. Therefore, the horizontal loop stiffness of the high-precision centerless grinding machine could be increased by about 15% by introducing a concrete-filled bed.

The displacement of the RW caused by the horizontal grinding force was greater than that of the GW due to the pitch error of the RW feed table, as shown in Fig. 11(b). As a result, a countermeasure to reduce the pitch error of the RW feed table is required to increase the horizontal loop stiffness of the high-precision centerless grinding machine.

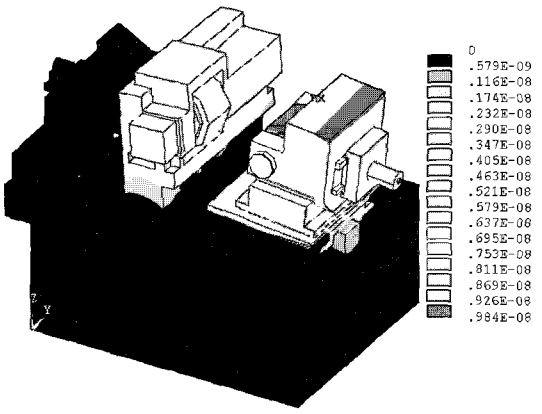

Fig. 11(a) Structural deformation of the virtual prototype due to a unit horizontal grinding force

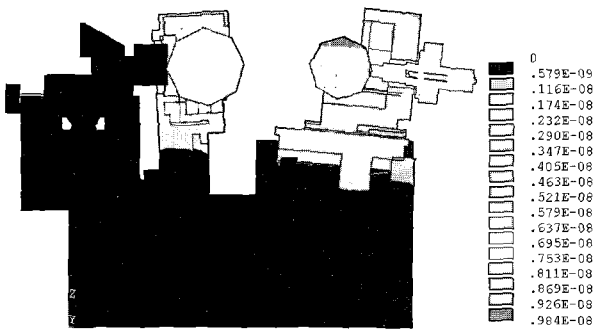

Fig. 11(b) Sectional view of the structural deformation

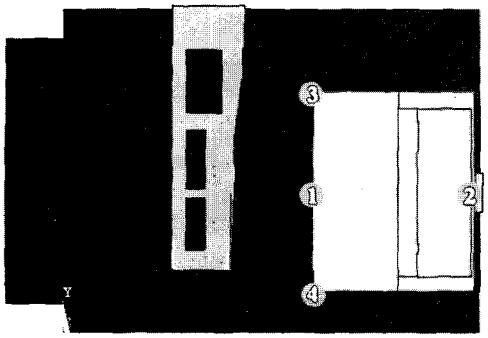

Fig. 12 Measurement points of the RW feed table (sectional view)

Table 7 Displacement of the RW feed table

Point	Concrete-filled bed		Unfilled bed	
	Axial	Vertical	Axial	Vertical
1	0.0036 μm	0.0027 μm	0.0041 μm	0.0031 μm
2	0.0036 μm	–0.0025 μm	0.0041 μm	–0.0026 μm
3	0.0036 μm	0.0026 μm	0.0041 μm	0.0030 μm
4	0.0036 μm	0.0026 μm	0.0041 μm	0.0030 μm

0.0082 μm, respectively, for the concrete-filled bed. Thus, the horizontal loop stiffness was 83.3 μm/N. With the unfilled bed, the horizontal displacement of the GW and RW were –0.0048 μm and

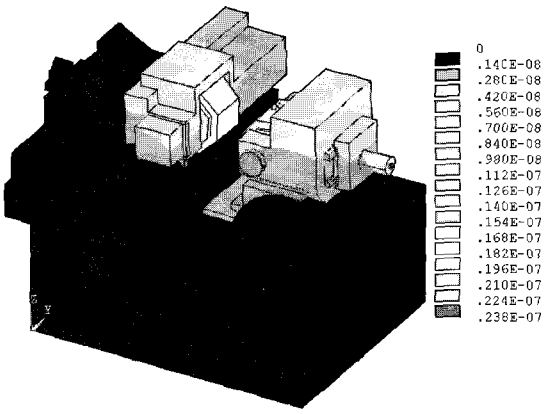

Fig. 13(a) Structural deformation of the virtual prototype due to a unit vertical grinding force

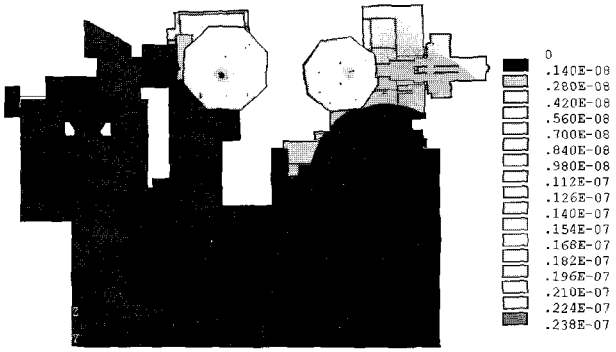

Fig. 13(b) Sectional view of the structural deformation

3.2.3 Vertical Loop Stiffness

The vertical loop stiffness was estimated by analyzing the structural deformation when a vertical grinding force of 1 N in the opposition direction was applied to the center portion of the GW and RW. The structural deformation of the high-precision centerless grinding machine caused by the vertical grinding force is shown in Fig. 13. For the concrete-filled bed, the vertical displacement of the GW and RW were 0.0024 μm and –0.0037 μm, respectively, and the vertical loop stiffness was 163.9 μm/N. With the unfilled bed, the vertical displacement of the GW and RW were 0.0026 μm and –0.0038 μm, respectively, and the vertical loop stiffness was 156.3 μm/N. Therefore, the vertical loop stiffness of the high-precision centerless grinding machine could be increased by about 5% by introducing a concrete-filled bed.

4. Conclusions

In this study, a structural characteristic analysis and evaluation were performed using a virtual prototype of a high-precision centerless grinding machine to realize systematic design technology and performance improvements required to manufacture ferrules. The prototype consisted of a concrete-filled bed, hydrostatic GW and RW spindle systems, hydrostatic RW feed mechanism, RW swivel mechanism, and on-machine GW and RW dressers. By comparing

the structural characteristics of concrete-filled and unfilled beds, the study demonstrated that the use of a concrete-filled bed considerably improved the structural stiffness and accuracy of the high-precision centerless grinding machine. The following conclusions were drawn.

1) The upper gap of the hydrostatic guideway of the high-precision centerless grinding machine with the concrete-filled bed increased on average by 4.15 to 4.62 μm due to the bending deformation of the rails from the hydrostatic effects. The subsequent real vertical stiffness of the hydrostatic guideway was expected to become 865 N/μm (about 10%) less than the designed vertical stiffness of 960 N/μm. The increment in the upper gap of the hydrostatic guideway was reduced by about 20% by introducing a concrete-filled bed.
2) To minimize the position error of the RW, the mass center of the structural elements on the RW feed table must be coincident with the center of the table.
3) The deflections of the upper bed plate of the high-precision centerless grinding machine with the unfilled bed were approximately 100% and 150% greater in the longitudinal and transverse directions, respectively, than those of the machine with the concrete-filled bed. Thus, introducing a concrete-filled bed greatly contributed to an increased structural stiffness of the high-precision centerless grinding machine.
4) The pitch error of the RW feed table caused by the horizontal grinding force was reduced by about 10% by introducing a concrete-filled bed.
5) The RW feed system was designed as a well-balanced left–right symmetric structure since the yaw error of the RW feed table caused by a horizontal grinding force was extremely small.
6) The horizontal and vertical loop stiffness values of the high-precision centerless grinding machine with a concrete-filled bed were 83.3 μm/N and 163.9 μm/N, respectively, which were 15% and 5% greater compared to those of an unfilled bed.

ACKNOWLEDGEMENT

This research was supported by the Middle Term Stronghold Technology Development Program of the Korean Ministry of Commerce, Industry, and Energy.

REFERENCES

1. Rowe, W. B., Spraggett, S., Gill, R. and Davies, B. J., "Improvements in centreless grinding machine design," Annals of the CIRP, Vol. 36, No. 1, pp. 207-210, 1987.
2. Rowe, W. B., Miyashita, M. and Koenig, W., "Centerless grinding research and its application in advanced manufacturing technology," Annals of the CIRP, Vol. 38, No. 2, pp. 617-626, 1989.
3. Takeuchi, Y., Mitachi, S. and Nagase, R., "High-strength class-ceramic ferrule for SC-type single-mode optical fiber connector," IEEE Photonics Technology Letters, Vol. 9, No. 11, pp. 1502-1504, 1997.
4. Cho, S. J., Kim, H. G., Ebihara, T. and Tuskisima, H., "The study on the development of ultra precision centerless grinder," Journal of KSPE, Vol. 20, No. 6, pp. 11-14, 2003.
5. Lee, E. S., Cho, C. R. and Park, B. J., "Development of rotary diamond dressing system of centerless grinder for ferrule grinding," Journal of KSPE, Vol. 20, No. 6, pp. 15-19, 2003.
6. Park, C. H., Hwang, J. H. and Cho, S. J., "A study on the feeding system of centerless grinder for machining the ferrule," Proc. of KSPE, pp. 65-69, 2002.
7. Park, C. H., "Design and performance evaluation on the motion elements of centerless grinder," 3rd Mid-Evaluation Workshop of Intelligent Grinding System, 2004.
8. NSK, "Precision Machinery Product," NSK Catalog No. 3101, 1993.
9. THK, "Linear Motion System," THK Catalog No. 100-1K, 1991.